Original Article

Institution of MECHANICAL ENGINEERS
Journal of AUTOMOBILE ENGINEERING

Proc IMechE Part D:
J Automobile Engineering
1–15

DOI: 10.1177/0954407017728650
journals.sagepub.com/home/pid
SAGE

Variable caster steering in vehicle dynamics

Dai Q Vo[1,2], Hormoz Marzbani[1], Mohammad Fard[1] and Reza N Jazar[1,3]

Abstract

When a car is cornering, its wheels usually lean away from the centre of rotation. This phenomenon decreases lateral force, limits tyre performance and eventually reduces the vehicle lateral grip capacity. This paper proposes a strategy for varying caster in the front suspension, thereby altering the wheel camber to counteract this outward inclination. The homogeneous transformation was utilised to develop the road steering wheel kinematics which includes the wheel camber with respect to the ground during a cornering manoeuvre. A variable caster scheme was proposed based on the kinematic analysis of the camber. A rollable vehicle model, along with a camber-included tyre force model, was constructed. MATLAB/Simulink was used to simulate the dynamic behaviour of the vehicle with and without the variable caster scheme. The results from step steer, ramp steer, and sinusoidal steer inputs simulations show that the outward leaning phenomenon of the steering wheels equipped with the variable caster, is reduced significantly. The corresponding lateral acceleration and yaw rate increase without compromising other handling characteristics. The actively controlled car, therefore, provides better lateral stability compared to the passive car. The tyre kinematic model and the vehicle dynamic model were validated using multibody and experimental data.

Keywords

Variable caster, kinematics of steerable wheel, tyre performance, lateral acceleration, grip capacity

Date received: 20 September 2016; accepted: 11 July 2017

Introduction

The tyre's lateral force consists of the side-slip force and camber thrust,[1] as shown in Figure 1. Normally, when a car is negotiating a turn, the wheels lean outwards from the centre of rotation due to the roll motion of the body caused by centrifugal force and suspension geometry.[2] This phenomenon leads to a reduction in cornering force. The reduction becomes critical in high side-slip region where the side-slip force is saturated while much of available friction has not been utilised. Therefore, the cornering capacity of the vehicle is limited. Many efforts have been made to alter the camber in order to address this issue.[3–8] The research shows that camber control can improve vehicle stability, safety, and manoeuvrability in general while having some disadvantages. First, although motivated by using camber to maximise the tyre's lateral force, most of the research ended up with improving the vehicle performance in the range where the side-slip force is far from saturation.[3–5,8] In that range the side-slip force can still do the job well; and hence, controlling camber may not be as effective as that of steering angle. The second downside is that the controlled camber mechanism compromises with changing the suspension geometry such as roll centre,[3,4] which may badly affect vehicle dynamics. The mechanical complexity of the associated suspension system is another drawback of developing such systems.[6,7] Furthermore, in those investigations the camber gaining when the wheel is steering about the tilted kingpin axis has not been taken into account. This may lead to inaccuracy in computing the camber. As camber of a steered wheel can be altered by changing caster angle,[9–11] this research develops a method of varying caster for front steering wheels to minimise the outward leaning effect, thereby improving lateral grip capacity. The variable caster may also offset those above disadvantages.

[1]School of Engineering, RMIT University, Melbourne, Australia
[2]Faculty of Vehicle and Energy Engineering, Le Quy Don Technical University, Hanoi, Vietnam
[3]Xiamen University of Technology, Xiamen, China

Corresponding author:
Reza N Jazar, School of Engineering, RMIT University, GPO Box 2476, Melbourne, VIC 3001, Australia.
Email: reza.jazar@rmit.edu.au

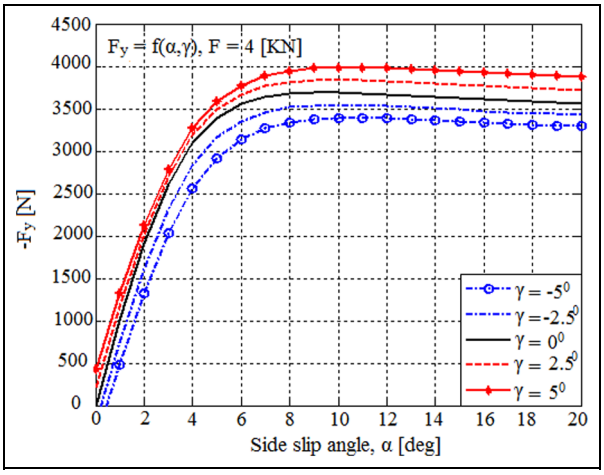

Figure 1. Cornering force consists of side-slip force and camber thrust.

We employed the homogeneous transformation as a tool to develop the kinematics of a steerable wheel. The ultimate camber in relation to the road (also called the inclination of the wheel with respect to the ground) was derived from the kinematics. An analysis of the camber was carried out to propose a strategy for varying the caster. A rollable model of the vehicle was built; and its dynamic response was produced by carrying out the simulation in MATLAB/Simulink environment. The simulation results show significant reduction in the outward inclination of the steering wheels, and improvement in lateral acceleration capacity.

Kinematics of a steerable tyre

Variable caster steering begins with the kinematics of a steerable wheel. First, we define coordinate systems sufficient to develop the kinematics of the wheel. The homogeneous transformation is then applied to map coordinates of an element between the coordinate systems. The kinematics is developed by expressing coordinates of elements in one of the coordinate frames.

Coordinate frames

To start with, a body coordinate frame $B(C_0xyz)$ is defined. It is the frame attached to the vehicle at the mass centre C_0, as depicted in Figure 2. The x-axis is longitudinal, going through C_0, and directed forwards. The y-axis goes laterally to the left of the drive's viewpoint. The z-axis is perpendicular to the ground and upwards so it makes the coordinate system a right-hand triad. It is also called B frame.

At each wheel, the four following frames shown in Figure 3 are also introduced. First, we define a tyre coordinate frame $T(x_t, y_t, x_t)$ that its origin is at the tyre-print centre. The x_t-axis is the intersection of the ground and tyre plane. The tyre plane is made by centrally narrowing the wheel into a flat disk. The z_t-axis is always vertical to the ground and upwards. The y_t-axis goes laterally to the left of the wheel and makes the system a right-hand triad. This frame only follows steering motion of the wheel.

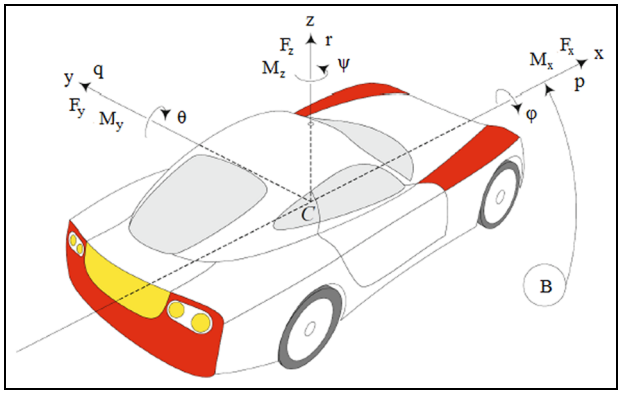

Figure 2. Body coordinate frame $B(C_0xyz)$.

We attach another frame called wheel coordinate frame $W(x_w, y_w, z_w)$ to the wheel. The origin of this W frame is also the wheel centre. The y_w is also the spin axis and towards left. The (x_wWz_w) plane is coincident with the tyre plane. When the wheel is steered with δ angle, the tyre plane makes a camber angle γ with the z_t. At zero steering angle, the x_w-axis is parallel to the x_t (they are no longer parallel if the wheel is steered). The z_w is determined such that it makes the W frame a right-hand triad coordinate system. An upright-wheel coordinate frame $W_0(x_{w0}, y_{w0}, z_{w0})$ is also stuck to the wheel. This W_0 frame is created by rotating the W frame an angle of $-\gamma_0$ about the x_t axis, at zero steering angle position of the wheel. Here, γ_0 is the static camber of the wheel, that is, the camber of the wheel when it is not steering, and the car is stationary. Note that both W and W_0 frames are attached to the wheel. Therefore, they follow every motion of the wheel except the spin. Finally, a wheel-body coordinate system $C(x_c, y_c, z_c)$ that coincides with the W_0 frame at zero steering angle position, is attached to the car body. The wheel-body coordinate frame is motionless with the car body and so it does not follow any motion of the wheel when steering.

As defined, the orientations and locations of the four coordinate frames are not affected by the spin motion of the wheel. Therefore, the spin is excluded from this kinematic analysis.

Homogeneous transformation and steering motion

We accept the assumption that the wheel is a flat and rigid disk throughout the analysis. In this section we initially assume that the wheel has zero static camber; and, the steering axis is a fixed line with respect to the car body. For generality of the kinematics, the last two assumptions will be removed in the next sections.

Because of the zero static camber, the W frame is coincident with the W_0 frame. Steering motion of the wheel can be equivalent to a δ-angle-rotation of the W frame, around the steering axis, with respect to the C frame. As the W frame initially coincides with the C

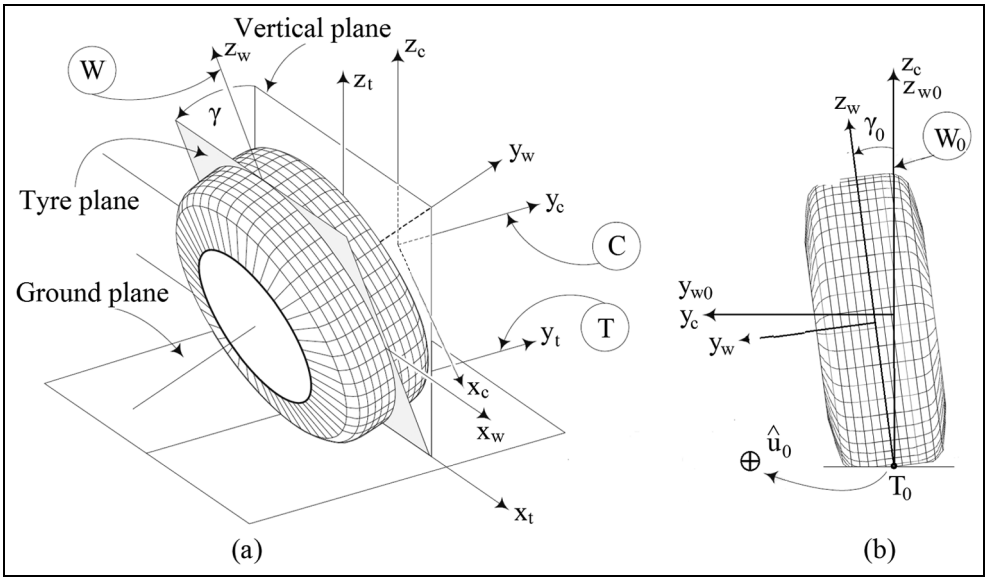

Figure 3. *T* frame, *W* frame, W_0 frame, and *C* frame: (a) The frames at δ position; (b) The W_0 frame coincides with the *C* frame at straight position.

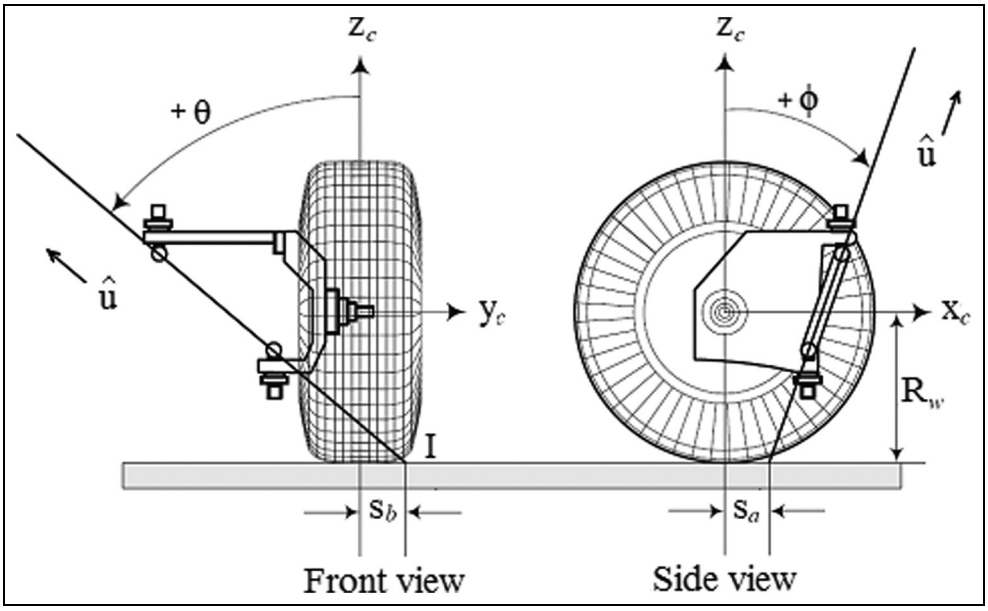

Figure 4. The orientation and location of the steering axis in the *C* frame.

frame (at zero steering angle), the transformation of coordinates between the two frames is described by the orientation and location of the steering axis, and the steering angle in the *C* frame.[9,12] The orientation and location of the steering axis are expressed by its direction unit vector $\hat{u}$, and a position vector d_I:[1,9]

$$\hat{u} = \begin{bmatrix} u_1 \\ u_2 \\ u_3 \end{bmatrix} = \frac{1}{\sqrt{cos^2\phi + cos^2\theta sin^2\phi}} \begin{bmatrix} cos\theta sin\phi \\ -sin\theta cos\phi \\ cos\theta cos\phi \end{bmatrix} \tag{1}$$

$$d_I = \begin{bmatrix} s_a \\ s_b \\ -R_w \end{bmatrix} \tag{2}$$

where ϕ is caster angle, θ is kingpin inclination angle (*KPI*), s_a is longitudinal location, s_b is lateral location and R_w represents the wheel radius, as shown in Figure 4.

Mapping coordinates in the wheel coordinate frame onto the wheel-body coordinate frame is governed by the homogeneous transformation:[9,12]

$$^{C}r = {}^{C}T_{W}{}^{W}r \tag{3}$$

where ${}^{C}r$ and ${}^{W}r$ are homogeneous representations of a position vector in the C frame and the W frame, respectively, i.e.

$$ {}^{C}r = \begin{bmatrix} {}^{C}x \\ {}^{C}y \\ {}^{C}z \\ 1 \end{bmatrix}; \quad {}^{W}r = \begin{bmatrix} {}^{W}x \\ {}^{W}y \\ {}^{W}z \\ 1 \end{bmatrix} \tag{4} $$

and ${}^{C}T_{W}$ is a 4×4 homogeneous matrix:

$$ {}^{C}T_{W} = \begin{bmatrix} R_{\hat{u},\delta} & d_I - R_{\hat{u},\delta} d_I \\ 0 & 1 \end{bmatrix} \tag{5} $$

where $R_{\hat{u},\delta}$ is called Rodriguez rotation formula, a 3×3 matrix for transforming between the two initially coincident frames with the rotation axis goes through the origin of the frames:[12]

$$ R_{\hat{u},\delta} = R(\hat{u}, \delta) \tag{6} $$

The homogeneous representation is used only for simplifying numerical calculations. The first three homogeneous coordinates of a position vector are still the same as the physical coordinates of the vector. Therefore, in this investigation, we still use the regular vector and its homogeneous representation equivalently.

Kinematics of a steerable tyre without static camber

By applying the homogenous transformation, we can determine coordinates of any element on the wheel (fixed to the W frame), expressed in the C frame. In this way, the kinematics of the wheel can be developed. Here we determine the kinematic camber, in relation to the car body, gaining when it is steered around the kingpin pivot.

By the sign conventions used in this analysis,[1] positive camber is determined as the angle γ that the tyre plane has rotated about the $+x_t$-axis from the vertical position (the wheel leans to the right as viewed from the rear regardless left or right wheel). A convenient way to compute the camber using the transformation is through calculating the angle ρ, as depicted in Figure 5, between the normal vectors of the tyre plane and the ground plane, as the following equation:

$$ \gamma = \frac{\pi}{2} - \rho \tag{7} $$

If the unit vectors in the directions of x_c, y_c and z_c of the C frame are denoted by $\hat{I}$, $\hat{J}$, and $\hat{K}$; and, the unit vectors in the directions of x_w, y_w and z_w of the W frame are symbolised by $\hat{i}$, $\hat{j}$, and $\hat{k}$, then ρ will be:

$$ \rho = acos \frac{{}^{C}\hat{j} \cdot {}^{C}\hat{K}}{\left|{}^{C}\hat{j}\right| \cdot \left|{}^{C}\hat{K}\right|} \tag{8} $$

where

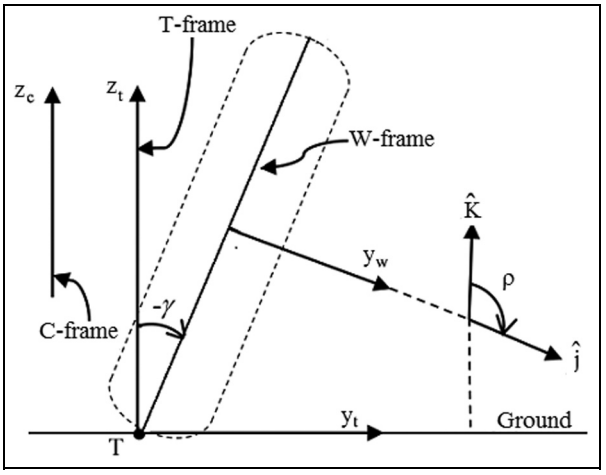

Figure 5. The front view of the steered wheel with the camber sign convention.

$$ {}^{C}\hat{K} = \begin{bmatrix} 0 \\ 0 \\ 1 \\ 0 \end{bmatrix} \tag{9} $$

$$ \begin{aligned} {}^{C}\hat{j} = {}^{C}T_{W}\,{}^{W}\hat{j} &= \begin{bmatrix} R_{\hat{u},\delta} & d_I - R_{\hat{u},\delta} d_I \\ 0 & 1 \end{bmatrix} \begin{bmatrix} 0 \\ 1 \\ 0 \\ 0 \end{bmatrix} \\ &= \begin{bmatrix} u_1 u_2 (1 - cos\delta) - u_3 sin\delta \\ u_2^2 (1 - cos\delta) + cos\delta \\ u_2 u_3 (1 - cos\delta) + u_1 sin\delta \\ 0 \end{bmatrix} \end{aligned} \tag{10} $$

By substituting equations (9) and (10) in equation (8) and then in equation (7), we have:

$$ \gamma = \frac{\pi}{2} - acos[u_2 u_3 (1 - cos\delta) + u_1 sin\delta] \tag{11} $$

If we substitute equation (1) in equation (11), the camber of a steered wheel will be:

$$ \begin{aligned} \gamma = \frac{\pi}{2} - acos[& \frac{cos\theta sin\phi}{\sqrt{cos^2\phi + cos^2\theta sin^2\phi}} sin\delta \\ & - \frac{cos^2\phi sin\theta cos\theta}{cos^2\phi + cos^2\theta sin^2\phi} vers\delta] \end{aligned} \tag{12} $$

As can be seen clearly in equation (12), the camber of a steered wheel only depends on the caster, and the *KPI*. Thus, the only way to indirectly control camber of a steered wheel is varying its steering axis orientation.

Kinematics of a steerable tyre with static camber

In the previous section, we assumed that the wheel had zero static camber. Therefore, the W coordinate frame coincided with the W_0 coordinate frame. It is more practical that the wheel has non-zero static camber.

This static camber, γ_0, is measured when the car is stationary and the wheel is not steering. This section develops the kinematics of such a steered wheel. As mentioned earlier, the W frame is actually created by rotating the W_0 frame an angle of γ_0 about the axis that coincides with the x_t-axis at straight position of the wheel. This is illustrated in Figure 3(b). The rotating axis is denoted by the direction unit vector $\hat{u}_0$, point T_0, both expressed in the W_0 coordinate frame:

$$^{W_0}\hat{u}_0 = \hat{u}_0 = \begin{bmatrix} 1 \\ 0 \\ 0 \end{bmatrix} \tag{13}$$

$$^{W_0}d_{T_0} = \begin{bmatrix} 0 \\ 0 \\ -R_w \end{bmatrix} \tag{14}$$

The homogeneous transformation matrix from the wheel coordinate frame W to the upright-wheel coordinate frame W_0 is written as:

$$\begin{aligned} {}^{W_0}T_W &= \begin{bmatrix} R_{\hat{u}_0,\gamma_0} & {}^{W_0}d_{T_0} - R_{\hat{u}_0,\gamma_0}{}^{W_0}d_{T_0} \\ 0 & 1 \end{bmatrix} \\ &= \begin{bmatrix} 1 & 0 & 0 & 0 \\ 0 & cos\gamma_0 & -sin\gamma_0 & -R_w sin\gamma_0 \\ 0 & sin\gamma_0 & cos\gamma_0 & R_w(cos\gamma_0 - 1) \\ 0 & 0 & 0 & 1 \end{bmatrix} \end{aligned} \tag{15}$$

Therefore, the coordinates of a point in the W frame can be transformed into those of the C frame by the two following transformations:

$$\begin{aligned} {}^{C}r &= {}^{C}T_{W_0}{}^{W_0}T_W{}^{W}r \\ &= \begin{bmatrix} R_{\hat{u},\delta} & {}^{C}d_I - R_{\hat{u},\delta}{}^{C}d_I \\ 0 & 1 \end{bmatrix} {}^{W_0}T_W{}^{W}r \end{aligned} \tag{16}$$

To determine the camber using equations (7) and (8), the ${}^{W}\hat{j}$ needs to be transformed into ${}^{C}\hat{j}$ by the following equation:

$${}^{C}\hat{j} = {}^{C}T_{W_0}{}^{W_0}T_W{}^{W}\hat{j} = {}^{C}T_{W_0}{}^{W_0}T_W \begin{bmatrix} 0 \\ 1 \\ 0 \\ 0 \end{bmatrix} \tag{17}$$

Substituting equations (17) and (9) in equation (8), and then equation (8) in equation (7), we have:

$$\begin{aligned} \gamma = \frac{\pi}{2} - acos\{&[u_2u_3(1 - cos\delta) + u_1 sin\delta]cos\gamma_0 \\ &+ [u_3^2(1 - cos\delta) + cos\delta]sin\gamma_0\} \end{aligned} \tag{18}$$

Substituting equation (1) in equation (18) yields the camber of the steered wheel:

$$\begin{aligned} \gamma = \frac{\pi}{2} - acos\{&[\frac{cos\theta sin\phi}{\sqrt{cos^2\phi + cos^2\theta sin^2\phi}} sin\delta \\ &- \frac{cos^2\phi sin\theta cos\theta}{cos^2\phi + cos^2\theta sin^2\phi} vers\delta]cos\gamma_0 \\ &+ [\frac{cos^2\phi cos^2\theta}{cos^2\phi + cos^2\theta sin^2\phi} vers\delta + cos\delta]sin\gamma_0\} \end{aligned} \tag{19}$$

We can verify that, when $\gamma_0 = 0$, equation (19) reduces to equation (12).

Wheel camber with respect to the ground in cornering

The camber determined in the previous sections is measured in relation to the car body. The camber of wheel with respect to the ground, however, is the ultimate parameter for calculating the camber force. When a car negotiates a turn its body rolls. The roll motion causes change in the orientation of the steering axis, with respect to the ground. It also gives a rise to a change in *initial camber*– the camber of the wheel at zero steering position. (This camber is similar to the static camber mentioned earlier. It is not called static camber as the car now is not stationary. Therefore, hereafter we call it *initial camber*.) Furthermore, the wheel gains camber as it is steered about the tilted steering axis. Determining the ultimate camber of such a steering wheel starts with defining the dynamic orientation of the steering axis with respect to the ground. When the car is in roll motion, the dynamic kingpin inclination angle (*DKPI*), in relation to the ground, is:

$$\theta_D = \theta_S + \theta_\varphi = \theta + \theta_\varphi \tag{20}$$

where θ_S is the static kingpin inclination angle (*SKPI*) and also the design kingpin inclination angle; θ_φ is the inclination angle induced by the roll motion φ of the car body, as illustrated in Figure 6.

We assume that the roll motion does not alter the caster. This is due to the fact that the roll angle is small. Therefore, the dynamic caster, ϕ_D, is the same as its static value, ϕ_S:

$$\phi_D = \phi_S = \phi \tag{21}$$

The roll motion of the car body also creates a change in the initial camber. This dynamic initial camber is:

$$\gamma_{0D} = \gamma_0 + \gamma_{0\varphi} \tag{22}$$

where γ_0 is the static camber and $\gamma_{0\varphi}$ is the initial camber portion caused by the roll motion. Note that the additional *KPI* angle, θ_φ, and the initial camber portion, $\gamma_{0\varphi}$, both induced by the roll motion are the same:

$$\theta_\varphi = \gamma_{0\varphi} \tag{23}$$

In order to determine the wheel camber with respect to the ground, we now redefine the C frame to make it

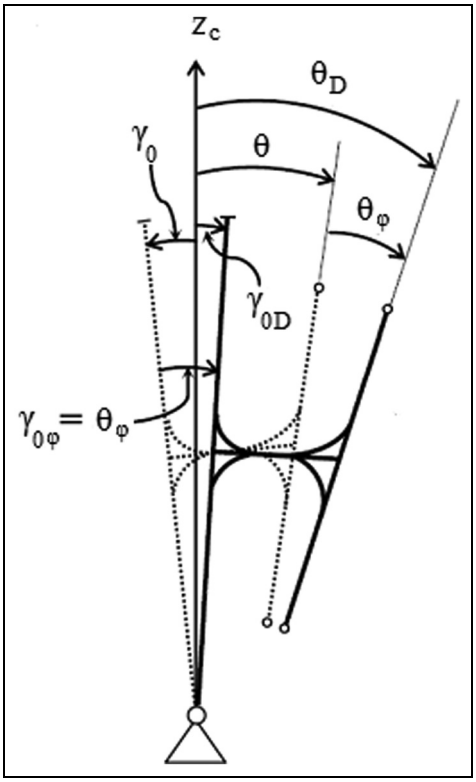

Figure 6. The change of steering axis and wheel camber in cornering.

always parallel to the ground during the turn. We introduce a new concept of no-roll-body. This no-roll-body is attached to the roll axis of the car body but it does not follow the roll motion. At the stationary position of the vehicle, we attach the C frame to the no-roll-body at the same position as it previously was. By definition, the C frame follows the horizontal motion of the car and is always parallel to the ground. Therefore, the orientation of the steering axis with respect to the ground is also in relation to the C frame. As camber of a steered wheel only depends on the steering pivot's orientation, the camber expressed in the new C frame is also that with respect to the ground.

Employing the homogeneous transformation method, transforming coordinates from the W frame into the C frame is governed by the following equation:

$$ {}^{C}r = {}^{C}T'_{W_0}\,{}^{W_0}T'_{W}\,{}^{W}r \tag{24} $$

where ${}^{C}T'_{W_0}$ and ${}^{W_0}T'_{W}$ are respectively similar to ${}^{C}T_{W_0}$ and ${}^{W_0}T_{W}$ but with the dynamic values of the parameters:

$$ {}^{C}T'_{W_0} = \begin{bmatrix} R_{\hat{u}_D,\delta} & {}^{C}d_{I_D} - R_{\hat{u}_D,\delta}\,{}^{C}d_{I_D} \\ 0 & 1 \end{bmatrix} \tag{25} $$

$$ {}^{W_0}T'_{W} = \begin{bmatrix} R_{\hat{u}_0,(\gamma_0+\theta_\varphi)} & {}^{W_0}d_{T_0} - R_{\hat{u}_0,(\gamma_0+\theta_\varphi)}\,{}^{W_0}d_{T_0} \\ 0 & 1 \end{bmatrix} \tag{26} $$

$\hat{u}_D$ and d_{I_D} in equation (25) are the direction unit vector and the position vector representing the dynamic steering axis in the C frame, which are similar to equations (1) and (2), respectively:

$$ \hat{u}_D = \frac{1}{\sqrt{cos^2\phi_D + cos^2\theta_D sin^2\phi_D}} \begin{bmatrix} cos\theta_D sin\phi_D \\ -sin\theta_D cos\phi_D \\ cos\theta_D cos\phi_D \end{bmatrix} \tag{27} $$

$$ d_{I_D} = \begin{bmatrix} s_{aD} \\ s_{bD} \\ -R_w \end{bmatrix} \tag{28} $$

Using the same method in the previous section, the ultimate camber of the wheel with respect to the ground in cornering manoeuvre can be determined by the following equation:

$$ \begin{aligned} \gamma_G = \frac{\pi}{2} - acos\{[&\frac{cos(\theta+\theta_\varphi)sin\phi}{\sqrt{cos^2\phi + cos^2(\theta+\theta_\varphi)sin^2\phi}} sin\delta \\ &- \frac{cos^2\phi sin(\theta+\theta_\varphi)cos(\theta+\theta_\varphi)}{cos^2\phi + cos^2(\theta+\theta_\varphi)sin^2\phi} vers\delta]cos(\gamma_0+\theta_\varphi) \\ &+ [\frac{cos^2\phi cos^2(\theta+\theta_\varphi)}{cos^2\phi + cos^2(\theta+\theta_\varphi)sin^2\phi} vers\delta + cos\delta]sin(\gamma_0+\theta_\varphi)\} \end{aligned} \tag{29} $$

As shown by equation (29), the camber in relation to the ground is a function of the orientation of the steering axis, the steering angle, the roll motion of the car body along with the suspension geometry, and the static camber. We can verify that when the static camber and the roll motion are not included, equation (29) reduces to equation (12).

Variable caster steering strategy

Equations (12), (19) and (29) show that both caster and *KPI* angle affect the camber of a steered wheel. In comparison with *KPI*, however, caster is much more effective to create the camber.[9–11,13] Therefore, caster is chosen to control the camber to lessen the outward leaning phenomenon of the front steering wheels. To reduce the time of calculation the camber function is simplified. To do that, it is first rewritten as:

$$ \begin{aligned} sin\gamma_G = [&\frac{cos(\theta+\theta_\varphi)sin\phi}{\sqrt{cos^2\phi + cos^2(\theta+\theta_\varphi)sin^2\phi}} sin\delta \\ &- \frac{cos^2\phi sin(\theta+\theta_\varphi)cos(\theta+\theta_\varphi)}{cos^2\phi + cos^2(\theta+\theta_\varphi)sin^2\phi} vers\delta]cos(\gamma_0+\theta_\varphi) \\ &+ [\frac{cos^2\phi cos^2(\theta+\theta_\varphi)}{cos^2\phi + cos^2(\theta+\theta_\varphi)sin^2\phi} vers\delta \\ &+ cos\delta]sin(\gamma_0+\theta_\varphi) \end{aligned} \tag{30} $$

This variable caster strategy is designed to work only in high speed cornering conditions with small steering angles. Therefore, the following small angle approximations are made:

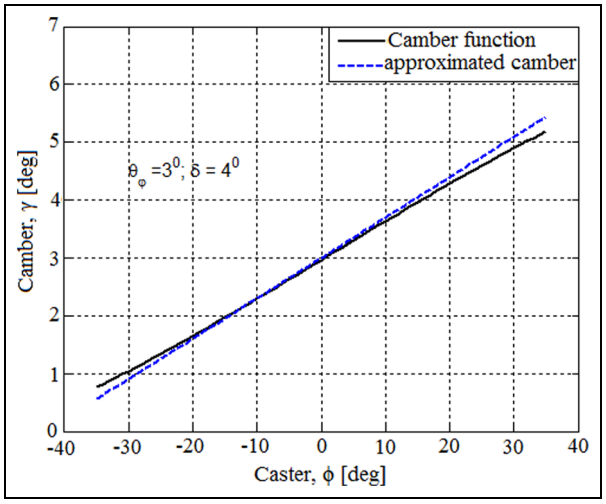

Figure 7. The approximated camber versus camber function.

$$\begin{aligned}
&\frac{cos(\theta + \theta_\varphi)}{\sqrt{cos^2\phi + cos^2(\theta + \theta_\varphi)sin^2\phi}} \approx 1 \\
&sin\delta \approx \delta \\
&cos\delta \approx 1 \\
&vers\delta = 1 - cos\delta \approx 0 \\
&cos(\gamma_0 + \theta_\varphi) \approx 1 \\
&sin(\gamma_0 + \theta_\varphi) \approx \gamma_0 + \theta_\varphi
\end{aligned} \tag{31}$$

The camber function is then reduced to:

$$\gamma_G = \phi\delta + \gamma_0 + \theta_\varphi \tag{32}$$

For practical ranges of the angles in equation (32), the error in using the approximation is less than 7%. Moreover, camber only contributes a minor part to the total lateral force. Therefore, the error and the approximated function are considered to be acceptable for this variable caster scheme. Figure 7 illustrates an exemplary comparison between the exact function and the approximated camber.

The approximated function shows that the camber of the wheel with respect to the ground in cornering manoeuvre can be controlled by the caster. As the aim of this research is to counter the outward inclination of the front steering wheels during a turn, the variable caster scheme is proposed such that the camber of the wheel is zero. Substituting $\gamma_G = 0$ in equation (32) yields:

$$\phi_{var} = -\frac{\gamma_0 + \theta_\varphi}{\delta} \tag{33}$$

Equation (33) suggests that the camber of the steerable wheel can mathematically be reduced to zero by controlling the caster based on the static camber γ_0, the *KPI* induced by roll motion $\theta_\varphi = \theta(\varphi)$, and the steering angle δ.

Since this investigation is to show the potential of variable caster steering, we do not focus on a particular car with a specific control algorithm. However, to show the effects of such a variable caster strategy on vehicle dynamics we examine the variable caster theory for an exemplary case: The vehicle is a front-wheel-steering car, has zero static camber ($\gamma_0 = 0$); and, the suspensions are equal length double A arm ($\theta_\varphi = \varphi$). The equation (33), therefore, reduces to:

$$\phi_{var} = -\frac{\varphi}{\delta} \tag{34}$$

Theoretically, if the caster is varied to satisfy equation (34), the camber of the wheel will be close to zero (rather than zero, because of the approximations made). However, the variable caster should be limited to be within a specific range. This is due to different constraints such as the required room for the steered wheel. Furthermore, when the vehicle is moving straight, a fixed caster similar to that of the original suspension should be used to assure the straight line stability. Considering all the above requirements, here we propose a strategy for varying caster:

$$\phi_{var} = \begin{cases} \phi_0 & \text{if } \delta = 0 \quad (35a) \\ \phi_0 & \text{if } \{\delta \neq 0,\ -\frac{\varphi}{\delta} > \phi_0\} \quad (35b) \\ \phi_1 & \text{if } \{\delta \neq 0,\ -\frac{\varphi}{\delta} < \phi_1\} \quad (35c) \\ -\frac{\varphi}{\delta} & \text{if } \{\delta \neq 0, \phi_1 \leqslant -\frac{\varphi}{\delta} \leqslant \phi_0\} \quad (35d) \end{cases}$$

where ϕ_0 and ϕ_1 are the maximum, and minimum values of the caster, respectively. Note that, by the sign conventions in this paper, the minimum caster is when the top end of the steering pivot leans rearwards maximum (and is negative).

In this investigation, we choose ϕ_0 as the fixed caster value of the original car. Therefore, when the car is not cornering its dynamic behaviour stays the same as that of the original car. The car with the variable caster only works differently when it negotiates a turn. We also choose ϕ_1 as the minimum achievable value of the caster required by the available room for steering wheel. The effect of the variable caster strategy on the lateral dynamics of the car will be examined by using the vehicle model presented in the next section.

Vehicle modelling

In order to investigate the dynamic performance of a car with and without the variable caster, a nonlinear dynamic model of the car (*NLDM*) is employed. The main characteristics which affect the lateral dynamics of a turning car, such as roll motion and load transfer, must be included. Therefore, a car model consisting of longitudinal, lateral, yaw and body roll motions of the vehicle, as shown in Figure 8, is adopted. To take the camber contribution and the non-linear characteristics of the tyre into account, we utilise the Magic Formula for tyre modelling.[14] For the simplicity of the analysis, however, the longitudinal velocity is assumed to be constant; the effects of body pitch and heave are neglected; we also assume that the car runs on a flat rigid ground.

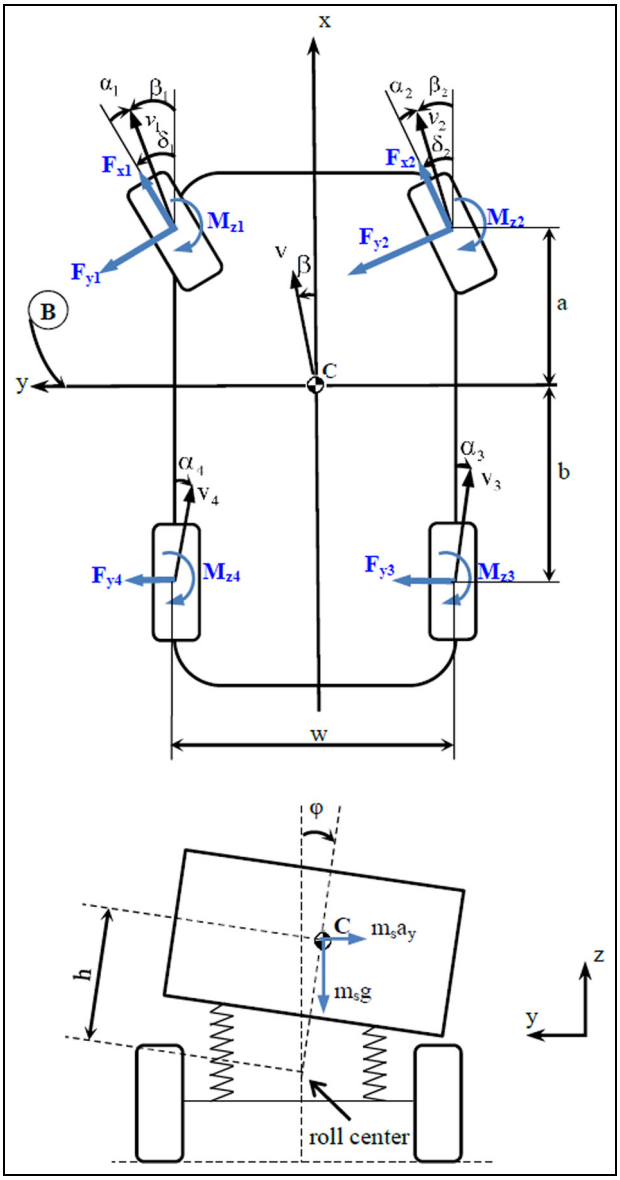

Figure 8. Nonlinear rollable vehicle model.

The lateral dynamics of the vehicle is governed by the equations of motion, expressed in the body coordinate frame:

$$m(\dot{v}_x - rv_y) + m_s h\dot{r}\varphi = F_x \tag{36}$$

$$m(\dot{v}_y + rv_x) - m_s h\ddot{\varphi} = F_y \tag{37}$$

$$I_{zz}\dot{r} + I_{xz}\ddot{\varphi} = M_z \tag{38}$$

$$I_{xx}\ddot{\varphi} + I_{xz}\dot{r} - m_s h(\dot{v}_y + rv_x) = M_x \tag{39}$$

The external forces and moments acting on a rigid car body are:

$$F_x = -F_{y1}sin\delta_1 - F_{y2}sin\delta_2 + F_{x1}cos\delta_1 + F_{x2}cos\delta_2 \tag{40}$$

$$F_y = F_{y1}cos\delta_1 + F_{y2}cos\delta_2 + F_{x1}sin\delta_1 + F_{x2}sin\delta_2 + F_{y3} + F_{y4} \tag{41}$$

$$M_z = (M_{z1} + M_{z2} + M_{z3} + M_{z4}) + a(F_{y1}cos\delta_1 + F_{y2}cos\delta_2) + a(F_{x1}sin\delta_1 + F_{x2}sin\delta_2) + \frac{w}{2}(F_{y1}sin\delta_1 - F_{y2}sin\delta_2) - \frac{w}{2}(F_{x1}cos\delta_1 - F_{x2}cos\delta_2) - b(F_{y3} + F_{y4}) \tag{42}$$

$$M_x = m_s ghsin\varphi - (K_{\varphi 1} + K_{\varphi 2})\varphi - (C_{\varphi 1} + C_{\varphi 2})\dot{\varphi} \tag{43}$$

where F_{xi}, F_{yi}, and M_{zi} are tyre longitudinal, lateral forces and moment at the wheel number i. The tyre lateral force, and moment are modelled using the Magic Formula:[14]

$$F_{yi} = F_{yi}(\mu_i, F_{zi}, \alpha_i, \gamma_i); i = 1.4 \tag{44}$$

$$M_{zi} = M_{zi}(\mu_i, F_{zi}, \alpha_i, \gamma_i); i = 1.4 \tag{45}$$

where μ_i is the road–tyre friction coefficient at the tyre number i, F_{zi} is the normal force of the tyre number i and is a function of longitudinal, lateral accelerations and the roll motion:

$$F_{z1} = \frac{mgb}{2L} - \frac{mh_g}{2L}a_x - \frac{a_y}{w}\left(\frac{m_s b_s h_f}{L} + m_{uf}h_{uf}\right) - \frac{1}{w}(K_{\varphi 1}\varphi + C_{\varphi 1}\dot{\varphi}) \tag{46}$$

$$F_{z2} = \frac{mgb}{2L} - \frac{mh_g}{2L}a_x + \frac{a_y}{w}\left(\frac{m_s b_s h_f}{L} + m_{uf}h_{uf}\right) + \frac{1}{w}(K_{\varphi 1}\varphi + C_{\varphi 1}\dot{\varphi}) \tag{47}$$

$$F_{z3} = \frac{mga}{2L} + \frac{mh_g}{2L}a_x + \frac{a_y}{w}\left(\frac{m_s a_s h_r}{L} + m_{ur}h_{ur}\right) + \frac{1}{w}(K_{\varphi 2}\varphi + C_{\varphi 2}\dot{\varphi}) \tag{48}$$

$$F_{z4} = \frac{mga}{2L} + \frac{mh_g}{2L}a_x - \frac{a_y}{w}\left(\frac{m_s a_s h_r}{L} + m_{ur}h_{ur}\right) - \frac{1}{w}(K_{\varphi 2}\varphi + C_{\varphi 2}\dot{\varphi}) \tag{49}$$

α_i is the side-slip angle of the tyre number i:

$$\alpha_1 = \delta_1 - tan^{-1}\frac{v_y + ar}{v_x - \frac{w}{2}r} \tag{50}$$

$$\alpha_2 = \delta_2 - tan^{-1}\frac{v_y + ar}{v_x + \frac{w}{2}r} \tag{51}$$

$$\alpha_3 = -tan^{-1}\frac{v_y - br}{v_x + \frac{w}{2}r} \tag{52}$$

$$\alpha_4 = -tan^{-1}\frac{v_y - br}{v_x - \frac{w}{2}r} \tag{53}$$

and γ_i is the camber of the wheel number i with respect to the ground, expressed by equation (29).

Vehicle dynamics with variable caster steering

A sedan car that has been parameterised is chosen for examining the potential of the variable caster strategy.[15,16] The dynamic responses of the vehicle to three types of steering inputs: step steer, ramp steer, and

Table 1. Vehicle parameters.

Parameter	Value	Parameter	Value
$m(kg)$	1705	$h(m)$	0.445
$m_s(kg)$	1527	$L(m)$	2.69
$m_{uf}(kg)$	98.1	$a(m)$	1.035
$m_{ur}(kg)$	79.7	$a_s(m)$	1.015
$I_{xx}(kgm^2)$	440.9	$w(m)$	1.535
$I_{xz}(kgm^2)$	21.09	$R_w(m)$	0.313
$I_{zz}(kgm^2)$	3048	$K_{\varphi 1}(\frac{Nm}{rad})$	47298
$h_g(m)$	0.542	$K_{\varphi 2}(\frac{Nm}{rad})$	37311
$h_f(m)$	0.13	$C_{\varphi 1}(\frac{Nms}{rad})$	2823
$h_r(m)$	0.11	$C_{\varphi 2}(\frac{Nms}{rad})$	2653
$h_{uf}(m)$	0.313	$\phi_0(deg)$	-5
$h_{ur}(m)$	0.313	$\phi_1(deg)$	-35

sinusoidal steer, are examined to evaluate handling performance in terms of steady state, limit, and transient behaviour. The vehicle parameters used for the simulation are presented in Table 1.

Step steer input

Step steer input is a manoeuvre used to assess both steady state and transient behaviours of a car. In this investigation, a rounded step steering input function to reach 0.1 radians in 1.5 s at the car velocity of 60 km/h was selected for the simulation. Figure 9 shows time histories of the steering input and responses of the vehicle in two cases: the benchmark configuration and the controlled caster. As can be seen in the Figure, the car's responses experience a transition from straight-running to steady state turning where the variables are constant. To be more specific, when the variable caster is applied, the steady state cambers of both inner and outer wheels

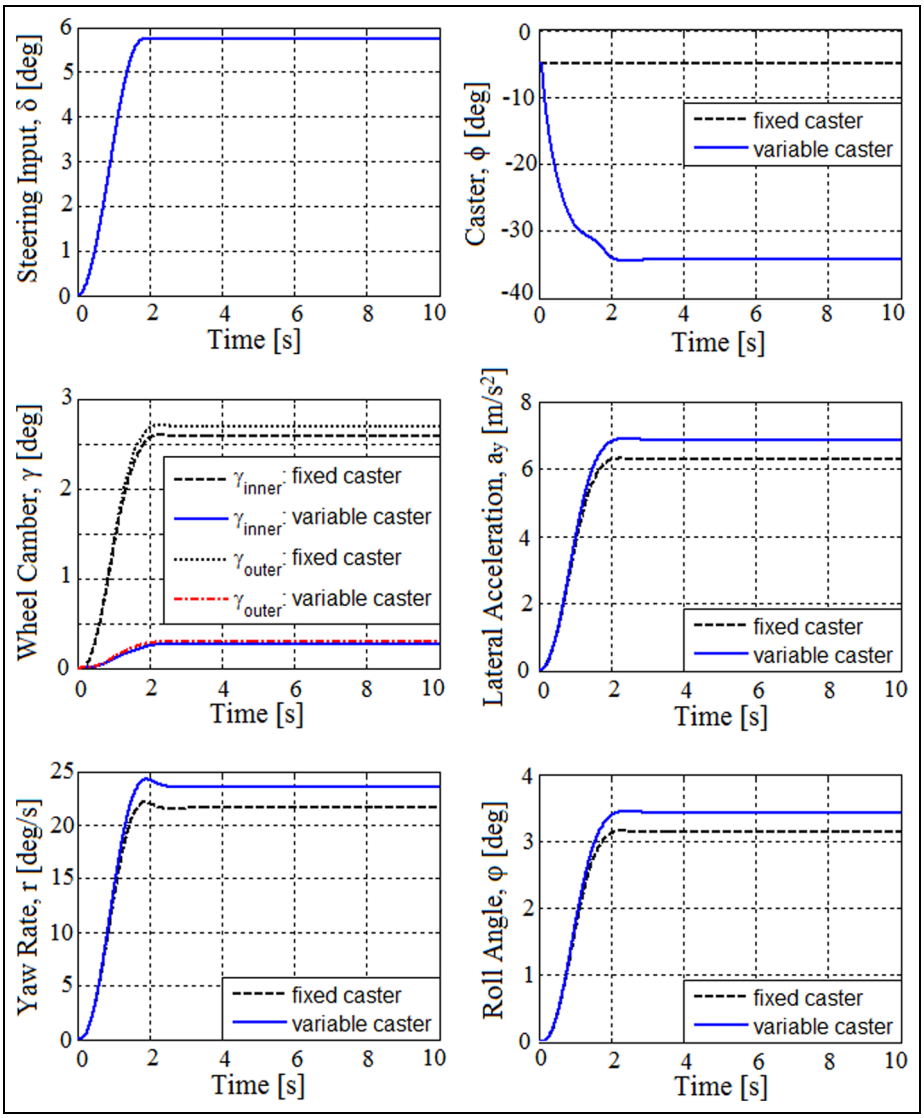

Figure 9. Vehicle responses to step steer input at 60 km/h.

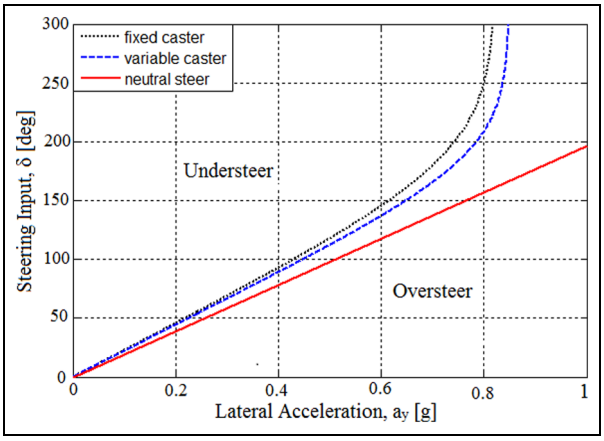

Figure 10. Steering angle versus lateral acceleration.

reduce by about 90%. This means, the wheels' outward inclinations are greatly lessened. As a result, the steady-state lateral acceleration of the car with variable caster increases to nearly 6.8 m/s^2 from the reference value of about 6.3 m/s^2. The steady state values of yaw rate and roll angle also experience increases of around 7% each. The transient characteristics such as overshoot value, settling time, and response time, however, are almost not affected by the variable caster. This is considered to be an upside of the variable caster strategy.

The controlled caster car, however, is expected to experience an increasing tendency towards oversteer. This is because the front wheels, with less outward inclinations, produce more lateral forces which are equivalent to larger front cornering stiffnesses compared to those of the reference vehicle. If the controlled car has oversteer characteristics, its stability will be impaired. The stability of a car is indicated by handling characteristics in terms of understeer, neutral steer or oversteer. Therefore, while the increase in the steady state acceleration is identified this response cannot be used to determine the stability of the car. To assess the change in the understeer gradient, simulation constant speed tests[17] were also carried out. Figure 10 shows the handling characteristics of the vehicle with and without the controlled caster, compared with the neutral steer line.[18] The graphs show that although there is a slight reduction in understeer tendency of controlled caster vehicle, the car in both cases has understeer characteristic. Furthermore, the trends of the two curves are the same: understeer gradient increases with lateral acceleration. The curves in Figure 10 also show that the maximum lateral acceleration of the controlled car is 0.85 g, an increase of about 5% from the benchmark. This increase along with the understeer characteristics show that the lateral grip capacity is improved without affecting the directional stability of the controlled car.

Ramp steer input

The steady state behaviour of the car is assessed through a ramp steer manoeuvre at the constant speed of 50 km/h. In this manoeuvre, the steering angle is gradually increasing to 10° in a period of 10 s. The steering input and the car's response to the steering are illustrated in Figure 11.

As can be observed, the lateral acceleration and the car body roll motion of the passive car increase with the steering angle. The roll motion causes the front wheels to lean away from the turn. The lean motion, however, is counteracted by the gained camber when the casters of the steered wheels are appropriately varied, resulting in very small positive cambers. The reduction of positive camber (leaning to the right – the outer side of the left turn) results in an improvement in lateral acceleration and yaw rate compared to the non-controlled car. As shown in Figure 11, the improvement is proportional to the steering angle. The controlled camber is not reduced to zero as a result of the approximations made in the previous section. As expected, there is also a slight difference between cambers of the left and the right wheels due to the existence of *KPI* in the configurations.

Sinusoidal steer input

Sinusoidal steer, a lane-change approximation, has been used by a number of organisations to evaluate vehicle dynamic performance as it is considered to be challenging to the vehicle's response and representative of actual driving situations. For that reason, in this investigation, a sinusoidal steer input shown in Figure 12(a) is applied to the vehicle. Figure 12(b) to (f) illustrates the responses of the vehicle. Generally speaking, the cambers of the controlled car reduce. Therefore, the associated lateral acceleration, yaw rate and roll angle increase. The increases in the controlled car's responses are maximum (around 7%) in the region near the curves' vertices. However, in the vicinity of steering-angle-zero-crossing points, the camber, and so the other responses of the controlled car almost do not change compared to those of the non-controlled case. This is due to the fact that, in that area, the steering input is near zero while the roll motion is still considerable (caused by a delay in the response). Therefore, the caster computed by equation (34) goes beyond the range $[\phi_0, \phi_1]$; and, hence, is set to ϕ_0 or ϕ_1 as in equation (35a), (35b) or (35c) which is depicted in the Figure 12(b). Despite this, the increase of lateral acceleration in the vertex-region gives the controlled car an advantage as improving the grip capacity is the aim of introducing such a variable caster.

Validation

Comparing simulation results with field test data is a good option for validating purpose. However, since this research is still in its theoretical stage the experiment data on the dynamic responses of the controlled caster vehicle has not been available. Therefore, the tyre

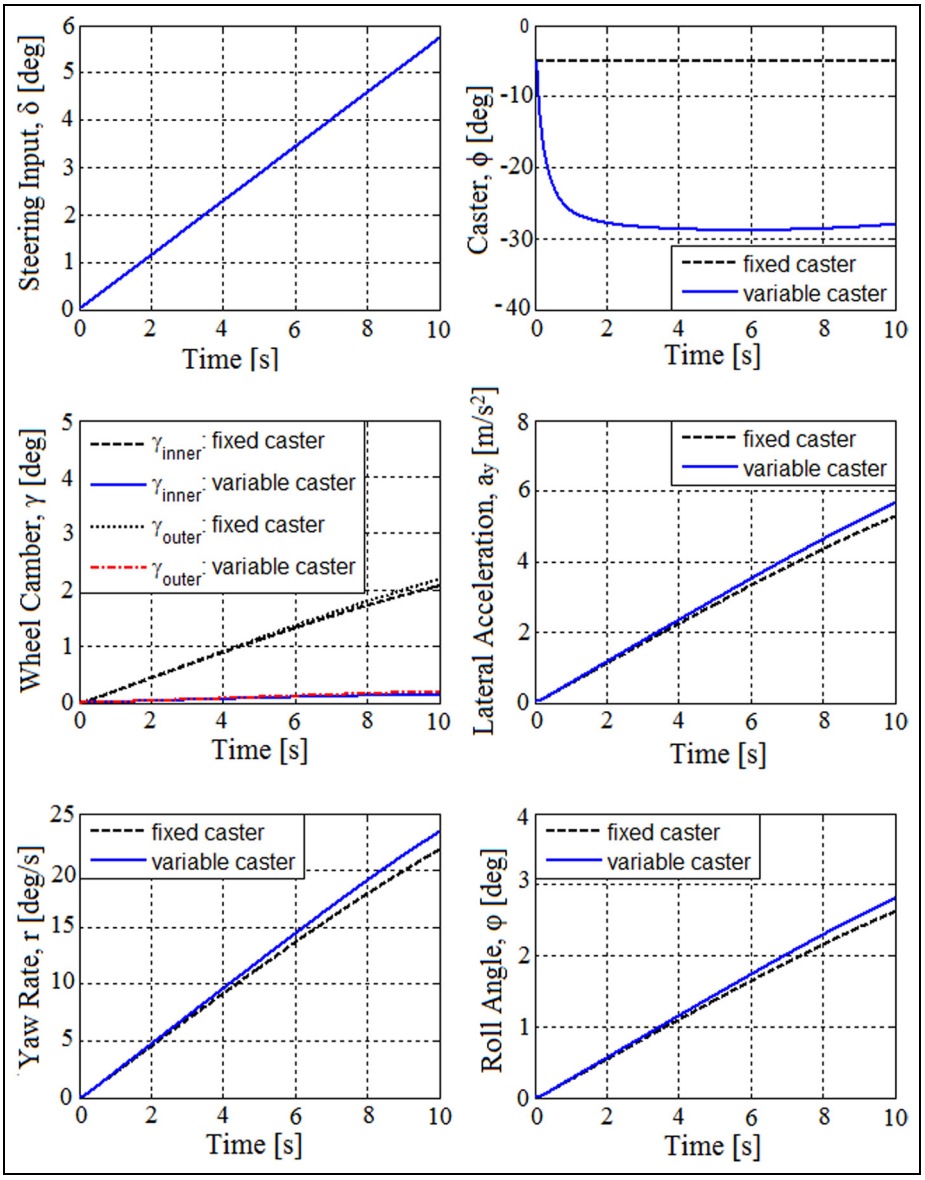

Figure 11. Vehicle responses to ramp steer input at 50 km/h.

kinematic model and the vehicle dynamic model developed in the research were validated separately.

Validation of tyre kinematics

To validate the tyre kinematics, a model of the rigid steerable wheel with adjustable caster and *KPI* angles was built using multibody software ADAMS. Parameters derived from the homogeneous transformation were compared with those from the multibody model.

Figure 13 illustrates how much the camber is generated using the homogeneous transformation method and ADAMS model for different orientations. We also compare the results with those developed by Alberding and Dixon.[13,19] For the sake of mathematical exactness, the comparison was made over the steering angle range from 0° to 360°, which is much greater than for practical steering angles.

It can clearly be seen that, there is no difference between the generated camber values derived from the homogeneous transformation method and the multibody model for different steering pivot's orientations. By contrast, the gained camber using Alberding formula and Dixon formula only show good agreement with that of the multibody model when there is no *KPI* angle or the steering angle is very small;[13,19] when there is a *KPI* angle and the steering angle is relatively large the camber values significantly differ from the multibody data. The comparison convinces that the kinematics of the steered wheel developed here using the homogeneous transformation is mathematically correct. Therefore, it is applicable to the development of variable caster theory.

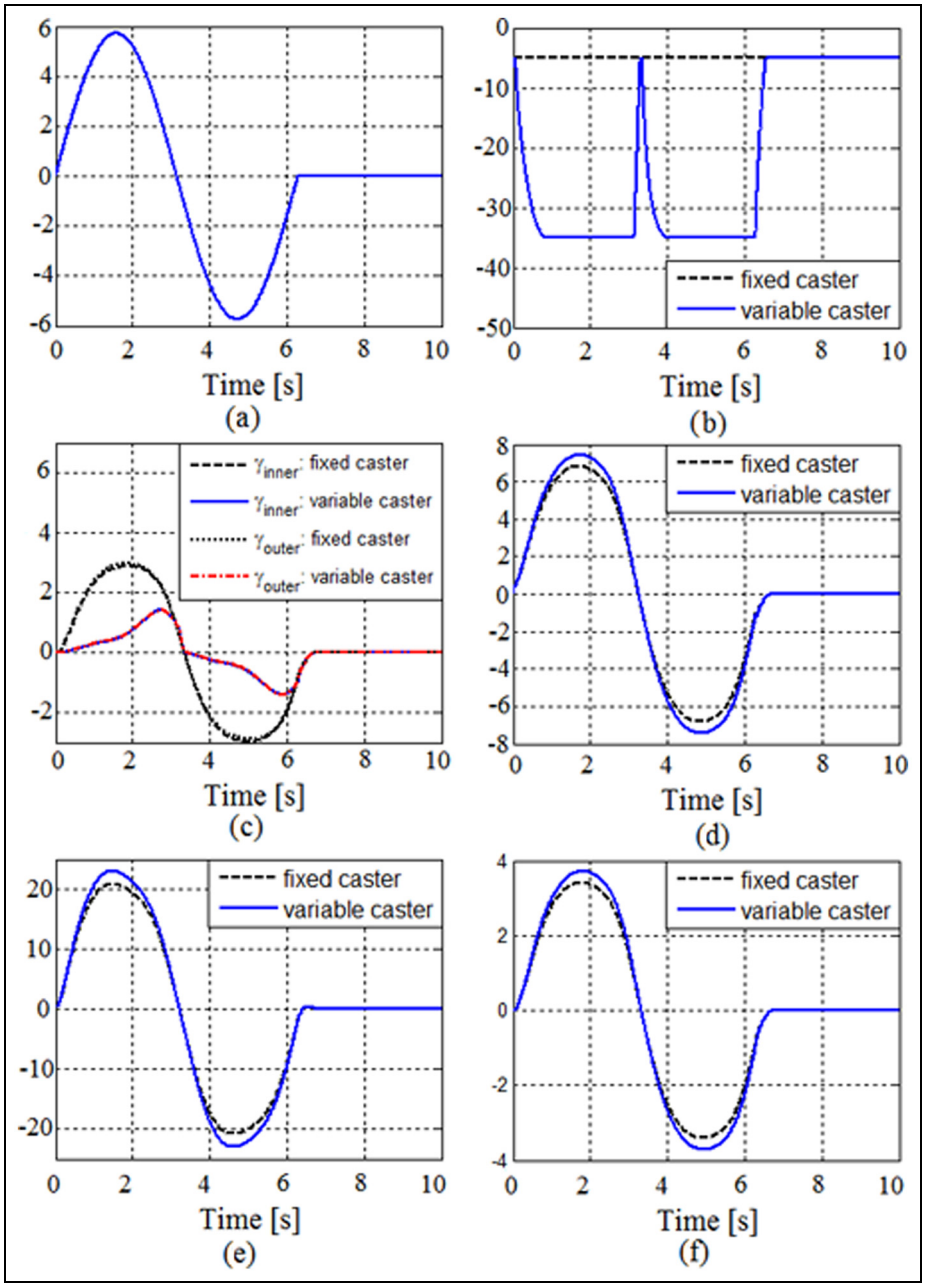

Figure 12. Vehicle responses to sinusoidal steer input at 70 km/h.

Validation of vehicle dynamics

Since the theoretical study presented here does not focus on one particular car, it is quite difficult to obtain both parameters and full test data from a specific car. Therefore, we utilised the publicly available data for 1994 Ford Taurus GL sedan car to conduct the validation of the *NLDM*.[15,16] The simulations utilised the actual measured steering wheel angle and car speed from the experiment.[15,16] The responses of the car to three types of steering input: slowly increasing steer, J-turn, and lane change manoeuvre, were compared for *NLDM*, and experiment data. They are shown in Figures 14–18.

More specifically, Figure 14 illustrates the vehicle behaviour when the inputs are slowly increasing steer at the constant speeds of 40 and 80 km/h.[15,16] The slowly increasing steer manoeuvre is used to evaluate the ability of a model to predict the steady state gain of the car for the whole range of lateral acceleration (from very low to limit). It is shown that simulation results are in good agreement with those of experiments. There is, however, a slightly difference between the simulation and the field test data at the limit. This may be attributed by the difference between the friction coefficient used in the model and the actual friction in the experiment.

J-turn manoeuvre is utilised to determine both steady state and transient responses of the car. The responses of the vehicle to J-turn steering inputs at 40 and 80 km/h[15] are depicted in Figures 15 and 16,

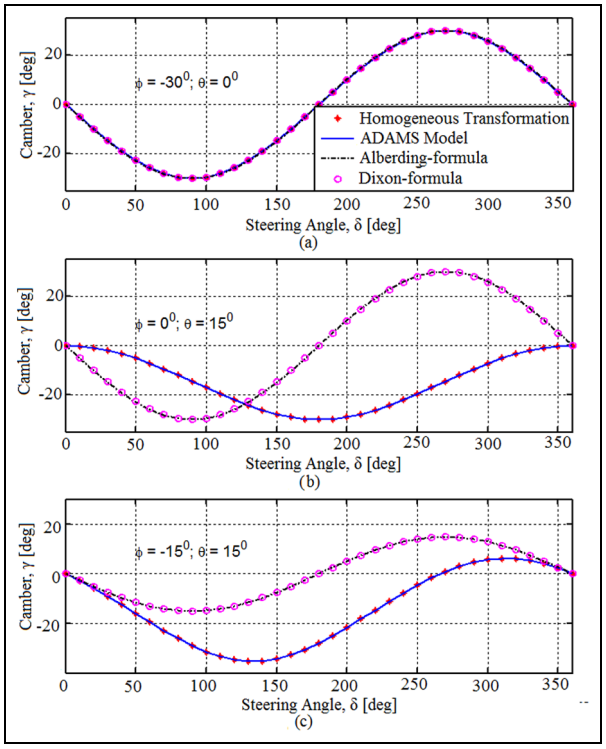

Figure 13. Camber generated for different caster ϕ, and *KPI* angle θ.

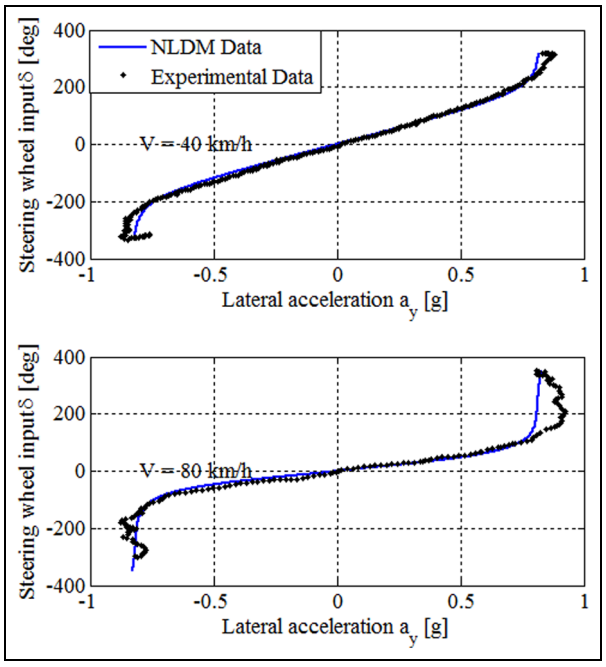

Figure 14. Lateral acceleration gain at 40 km/h and 80 km/h.

respectively. As can be seen from the graph, three is a good correlation between the simulation and the real vehicle, with the simulation results are slightly higher than the actual data. The *NLDM* developed in this investigation appears to be able to predict the vehicle response very well, especially for the case of 80 km/h.

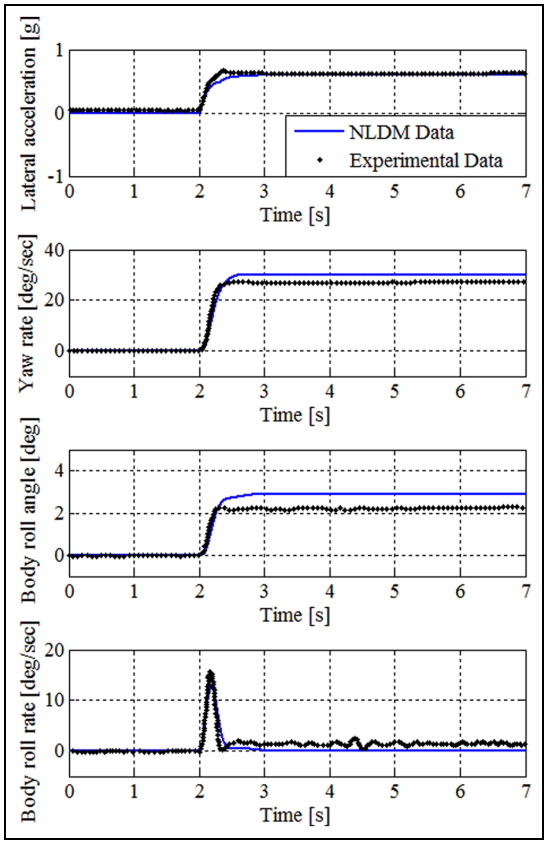

Figure 15. Vehicle responses to J-turn input at 40 km/h.

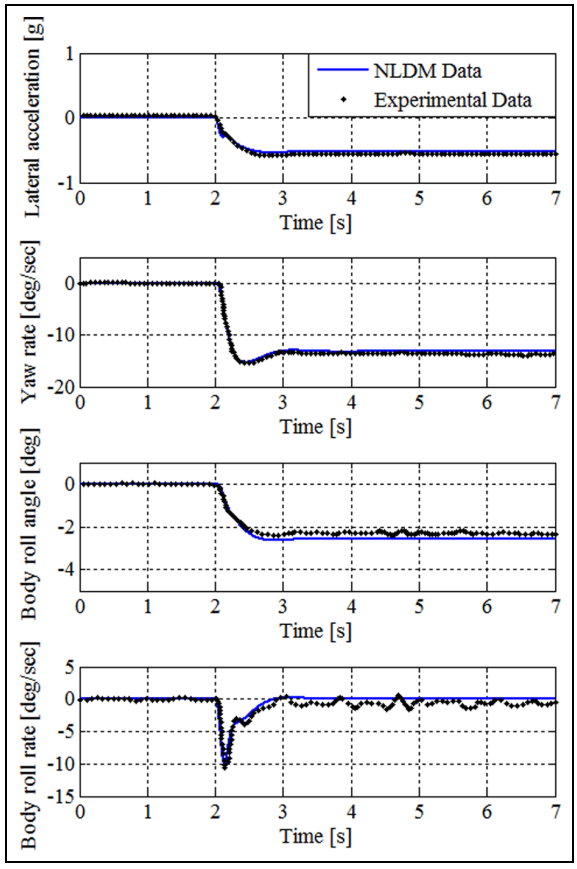

Figure 16. Vehicle responses to J-turn input at 80 km/h.

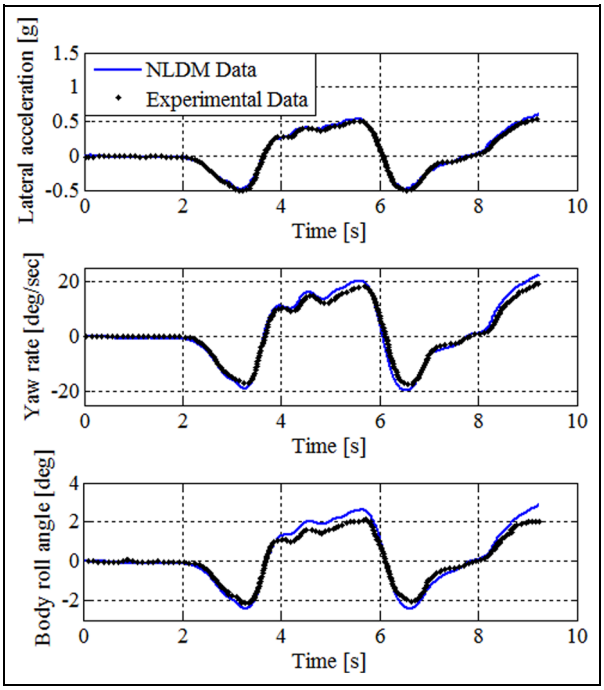

Figure 17. Vehicle responses to DLC input at 56 km/h.

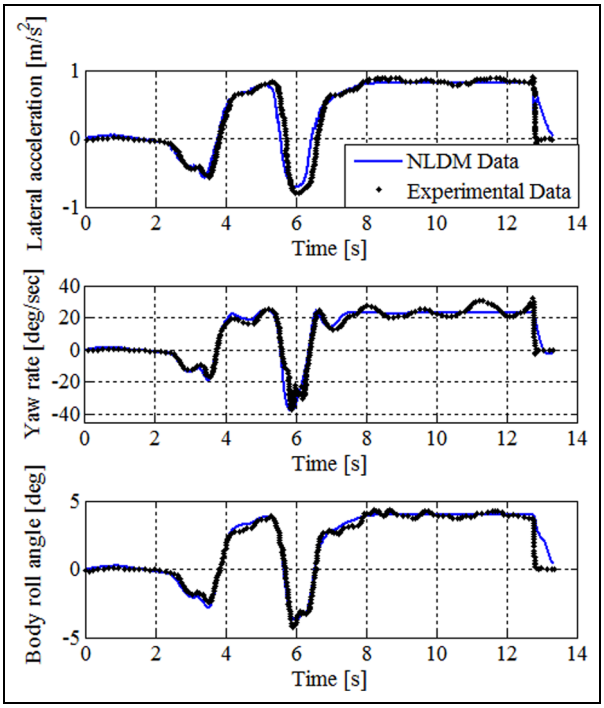

Figure 18. Vehicle responses to DLC input at 72 km/h.

The comparison between the simulation and actual vehicle was also made for double lane change manoeuvre which is considered to be representative of actual driving. This manoeuvre was performed at two constant speeds: 56 km/h (Figure 17) and 72 km/h (Figure 18).[15,16] The comparison shows that the *NLDM* does a good job in predicting the response of the vehicle for both speeds with a slightly better match for the speed of 72 km/h.

Conclusion

It is shown that the outward inclination of wheels in a turn can be lessened by varying the caster. Therefore, the lateral acceleration is increased. When the lateral force due to side-slip angle saturates, the lateral acceleration limit of the vehicle can still increase by altering the lateral force due to the camber. The camber can be controlled by a variable caster strategy. The kinematic analysis shows how these angles are related by the steering axis orientation. The rollable car model, along with typical steering manoeuvres, was used for assessing the performance of the car with and without the variable caster. The simulation results demonstrate that the lateral acceleration of caster-controlled car is improved while other handling characteristics such as understeer gradient, response time, overshoot and settling time are hardly sacrificed. The grip capacity is expanded by approximately 5% by utilising the variable caster which can potentially save lives by keeping the car on the road.

Declaration of conflicting interest

The author(s) declared no potential conflicts of interest with respect to the research, authorship, and/or publication of this article.

Funding

The author(s) received no financial support for the research, authorship, and/or publication of this article.

References

1. Jazar R. *Vehicle dynamics*. 2nd ed. New York: Springer, 2014.
2. Reimpell J, Stoll H and Betzler JW. Wheel travel and elastokinematics. In: Reimpell J, Stoll H and Betzler JW (eds) *The automotive chassis*. 2nd ed. Oxford: Butterworth-Heinemann, 2000, pp.149–265.
3. Park SJ and Sohn JH. Effects of camber angle control of front suspension on vehicle dynamic behaviors. *J Mech Sci Technol* 2012; 26: 307–313.
4. Nemeth B and Gaspar P. Control design of variable-geometry suspension considering the construction system. *IEEE Trans Veh Technol* 2013; 62: 4104–4109.
5. Kuwayama I, Baldoni F and Cheli F. Development of a control strategy for a variable camber suspension. *Int J Mech Control* 2007; 8: 38–52.
6. Laws SM. *An active camber concept for extreme maneuverability: mechatronic suspension design, tire modeling, and prototype development*. PhD Thesis, Stanford University, 2010.
7. Cuttino JF, Shepherd JS and Sinha MN. Design and development of an optimized, passive camber system for vehicles. SAE paper 2008-01-2950, 2008.
8. Horiguchi M, Mizuno A, Jones M, et al. Active camber control F2012-G04-007. *Lect Notes Electr Eng* 2013; 198: 247–256.
9. Vo DQ, Jazar RN and Fard M. A comparison between caster and lean angle in generating variable camber. SAE paper 2015-01-0067, 2015.

10. Vo DQ, Marzbani H, Fard M, et al. Caster camber relationship in vehicles. In: Jazar NR and Dai L (eds) *Nonlinear approaches in engineering applications: advanced analysis of vehicle related technologies*. Switzerland, Cham: Springer International Publishing, 2016, pp.63–89.
11. Jazar R, Subic A and Zhang N. Kinematics of a smart variable caster mechanism for a vehicle steerable wheel. *Veh Syst Dyn* 2012; 50: 1861–1875.
12. Jazar R. *Theory of applied robotics: kinematics, dynamics, and control*. 2nd ed. Boston, MA: Springer, 2010.
13. Dixon JC. *Suspension geometry and computation*. Chichester, UK: John Wiley & Sons, Ltd, 2009.
14. Pacejka H. *Tire and vehicle dynamics*. Elsevier Science, 2012.
15. Demerly JD and Youcef-Toumi K. Non-linear analysis of vehicle dynamics (NAVDyn): a reduced order model for vehicle handling analysis. SAE paper 2000-01-1621, 2000.
16. Salaani M. *Development and validation of a vehicle model for the National Advanced Driving Simulator*. PhD Thesis, The Ohio State University, USA, 1996.
17. Gillespie TD. *Fundamentals of vehicle dynamics*. Warrendale, PA: Society of Automotive Engineers, 1992.
18. Dixon JC. Linear and non-linear steady state vehicle handling. *Proc IMechE Part D: J Automobile Eng* 1988; 202: 173–186.
19. Alberding MB, Onder CH, Sager F, et al. Variable caster steering. *IEEE Trans Veh Technol* 2014; 63: 1513–1529.

Appendix

Notation

a	distance from the CoG of the car to the front wheels
a_s	distance from the CoG of the sprung mass to the front wheels
$C(x_c, y_c, z_c)$	the wheel-body coordinate frame
$C_{\varphi 1}$	front roll stiffness
$C_{\varphi 2}$	rear roll stiffness
d_I	the position vector of the point I
$h_g(m)$	height of CoG of the car
h_f	height of the roll centre at front
h_r	height of the roll centre at rear
h_{uf}	height of front unsprung mass
h_{ur}	height of rear unsprung mass
h	roll radius
I_{zz}	yaw inertia of the car
I_{xx}	roll inertia of the car
I_{xz}	product inertia of the car
$\hat{I}, \hat{J}, \hat{K}$	the unit vectors in the directions of x_c, y_c, z_c of the C frame
$\hat{i}, \hat{j}, \hat{k}$	the unit vectors in the directions of x_w, y_w, z_w of the W frame
$\hat{i}_0, \hat{j}_0, \hat{k}_0$	the unit vectors in the directions of x_{w0}, y_{w0}, z_{w0} of the W_0 frame
KPI	kingpin inclination angle
$K_{\varphi 1}$	front roll damping coefficient
$K_{\varphi 2}$	rear roll damping coefficient
L	wheel base
m	total mass of the car
m_s	sprung mass
m_{uf}	front unsprung mass
m_{ur}	rear unsprung mass
R_w	tyre radius
${}^C r$	the homogeneous representation of a position vector in the C frame
${}^W r$	the homogeneous representation of a position vector in the W frame
${}^{W_0} r$	the homogeneous representation of a position vector in the W_0 frame
$R_{\hat{u},\delta}$	the Rodriguez rotation matrix
s_a	longitudinal location of kingpin pivot-ground intersection
s_b	lateral location of kingpin pivot-ground intersection
$T(x_t, y_t, z_t)$	the tyre coordinate frame
${}^C T_w$	the homogeneous transformation matrix
$\hat{u}$	the direction unit vector of the steering axis
${}^C\hat{u}$	the direction unit vector of the steering axis expressed in the C frame
$vers\delta$	$1 - sin\delta$
w	the car track
$W(x_w, y_w, z_w)$	the wheel coordinate frame
W_0 (x_{w0}, y_{w0}, z_{w0})	the upright-wheel coordinate frame
γ	camber angle
δ	steering angle
θ	kingpin inclination angle
ρ	the angle between the normal vectors of tire plane and ground plane
ϕ	caster angle
ϕ_0	maximum caster
ϕ_1	minimum caster